

VERIFICATION OF CECOR COEFFICIENT METHODOLOGY
FOR APPLICATION TO
PRESSURIZED WATER REACTORS
OF THE
MIDDLE SOUTH UTILITIES SYSTEM

Reviewed by: Steve Thompson
Manager, Reactor Physics Analysis Section

8/1/84
Date

Approved by: T.R. Schmitz
Director, Nuclear Engineering Department

8/1/84
Date

ABSTRACT

The purpose of this report is to demonstrate Middle South Services, Inc. capability to provide updates to the CECOR program for Arkansas Nuclear One - Unit 2 and Waterford - Unit 3. CECOR is a computer program for synthesizing three dimensional power distributions from incore detector readings that was purchased from Combustion Engineering by Arkansas Power & Light and Louisiana Power & Light. This report documents the MSS methodology for generating cycle dependent CECOR data library updates and quantifies the power distribution reliability factors for F_{xy} , F_r and F_q to be used with the MSS libraries. The reliability factors insure that there is a 95% probability that at least 95% of the true F_{xy} , F_r and F_q will be less than the F_{xy} , F_r and F_q measured by CECOR plus 6.92, 5.69 and 7.71%, respectively. The benchmark database included data from 4 cycles of 177 and 217 fuel assembly CE reactors.

PROPRIETARY DATA CLAUSE

This document is the property of Middle South Services, Inc. and contains proprietary information developed and owned by Middle South Services, Inc. and is transmitted in confidence and trust. Appendices C and D are proprietary. Other proprietary information is identified by .

TABLE OF CONTENTS

<u>CHAPTER</u>	<u>Page</u>
1. INTRODUCTION.	1-1
2. IN-CORE INSTRUMENTATION	2-1
3. CECOR POWER DISTRIBUTION CALCULATION.	3-1
4. CECOR LIBRARY GENERATION.	4-1
5. DETERMINATION OF MSS CECOR LIBRARY UNCERTAINTIES.	5-1
6. REFERENCES.	6-1

APPENDICES

APPENDIX A - DEFINITIONS OF TERMS.	A-1
APPENDIX B - POOLING METHODOLOGY.	B-1
APPENDIX C - COUPLING/MEASUREMENT ERRORS FOR 177 AND 217 FUEL ASSEMBLY PLANTS	C-1
APPENDIX D - ASSEMBLY AXIAL SYNTHESIS ERRORS FOR 177 AND 217 FUEL ASSEMBLY PLANTS	D-1

LIST OF TABLES

<u>TABLE</u>	<u>TITLE</u>	<u>PAGE</u>
5.2.1	ANO-2 CYCLE 1 CECOR STATEPOINTS.	5-8
5.2.2	ANO-2 CYCLE 2 CECOR STATEPOINTS.	5-9
5.2.3	ANO-2 CYCLE 3 CECOR STATEPOINTS.	5-10
5.2.4	217 FA CYCLE 1 CECOR STATEPOINTS	5-11
5.2.5	ANO-2 CYCLE 1 CECOR STATISTICS	5-12
5.2.6	ANO-2 CYCLE 2 CECOR STATISTICS	5-13
5.2.7	ANO-2 CYCLE 3 CECOR STATISTICS	5-14
5.2.8	217 FA CYCLE 1 CECOR STATISTICS.	5-15
5.3.1	ASSEMBLY AXIAL SYNTHESIS UNCERTAINTY	5-16
5.6.1	SUMMARY OF UNCERTAINTY COMPONENTS FOR CECOR PEAKING FACTORS.	5-25
5.6.2	COMBINED 95%/95% PROBABILITY CONFIDENCE LOWER TOLERANCE LIMITS FOR CORE PEAKING FACTORS MEASURED BY CECOR	5-26

LIST OF FIGURES

<u>FIGURE</u>	<u>TITLE</u>	<u>PAGE</u>
2.1	INSTRUMENT PATTERN, ARKANSAS NUCLEAR ONE - UNIT 2.	2-3
2.2	INSTRUMENT PATTERN, WATERFORD - UNIT 3	2-4
2.3	TYPICAL NEUTRON DETECTOR AND DETECTOR ASSEMBLY	2-5
2.4	RHODIUM EMITTER DECAY SCHEME.	2-6
2.5	IN-CORE INSTRUMENTATION WIRING DIAGRAM	2-7
4.1	SCHEMATIC OF CECOR LIBRARY GENERATION.	4-2
4.2	ASSEMBLY 15 COUPLING COEFFICIENT COMPARISON.	4-3
5.3.1	F _{xy} ASSEMBLY AXIAL SYNTHESIS ERROR.	5-19
5.3.2	F _r ASSEMBLY AXIAL SYNTHESIS ERROR	5-20
5.3.3	F _q ASSEMBLY AXIAL SYNTHESIS ERROR	5-21
5.4.1	ANO-2 CYCLE 2 BOC COMPARISON OF [PDQ PEAK PIN TO ASSEMBLY AVERAGE PIN POWER, ARO]	5-22
5.4.2	ANO-2 CYCLE 2 BOC COMPARISON OF [PDQ PEAK PIN TO ASSEMBLY AVERAGE PIN POWER, BK6 INSERTED.]	5-23
5.4.3	PIN PEAKING SYNTHESIS ERROR.	5-24

1.0 INTRODUCTION

The CECOR program (Reference 1) is an off-line computer program which synthesizes detailed three-dimensional assembly and peak pin power distributions from fixed incore detector signals. The purpose of this report is to describe the methodology used by Middle South Services (MSS) to generate input data libraries for the CECOR program and to quantify the CECOR power distribution uncertainty which results from the use of this methodology.

The CECOR uncertainty documented herein, supercedes those uncertainties estimated in the MSS Physics Topical (Reference 2) relating to core monitoring. Section two of this report describes the incore instrumentation for Arkansas Nuclear One - Unit 2 (ANO-2) and Waterford - Unit 3 (W-3). Section three describes the algorithms used by CECOR to synthesize the three-dimensional power distribution from the incore detector readings and the coefficient library. A precalculated library of coefficients is used in the power synthesis. Chapter four describes the generation of the coefficient libraries from data generated from the MSS reactor physics methods described in Reference 2. Section five provides a quantification of CECOR uncertainties using MSS generated libraries.

2.0 IN-CORE INSTRUMENTATION

The incore instrumentation at Arkansas Nuclear One - Unit 2 and Waterford Unit 3 consists of fixed self-powered rhodium detector strings, movable self-powered rhodium detectors and background detectors. Figures 2.1 and 2.2 give the layout of incore instrumentation for ANO-2 and W-3. Each fixed incore detector string consists of five detectors equally spaced axially over the active fuel height. Each detector string is centered in the large center water hole of an assembly.

THE CECOR power distribution is based only on the fixed incore detector readings. The movable detectors are used for detector cross calibration and the background detectors are used periodically to determine a background correction for the fixed self-powered rhodium detectors.

2.1 Fixed Rhodium Detectors

A typical rhodium detector consists of a rhodium emitter, insulation, a collector sheath and signal lead wire as shown in Figure 2.3. The emitter consists of 99.9% rhodium-103 which is surrounded by a Al_2O_3 insulator which is enclosed in an Inconel sheath. The detectors are 40cm in length and are centered at 10, 30, 50, 70, and 90% of active core height.

When the rhodium-103 in the detector absorbs a neutron, rhodium-104 is produced which decays through beta emission. The complete rhodium decay scheme is shown in Figure 2.4. The escape of beta particles from the emitter produces a low-level current. A measuring resistor is utilized to produce a measurable voltage as shown

in Figure 2.5. The voltage is amplified, then digitized by an analog to digital converter for use by the plant computer.

2.2 Fixed Detector Signal Reliability

The concerns of detector signal repeatability, signal-to-power linearity and background signal effects were evaluated in Reference 3 by Combustion Engineering, and will not be repeated here.

Figure 2.1

INSTRUMENT PATTERN
ARKANSAS NUCLEAR ONE - UNIT 2

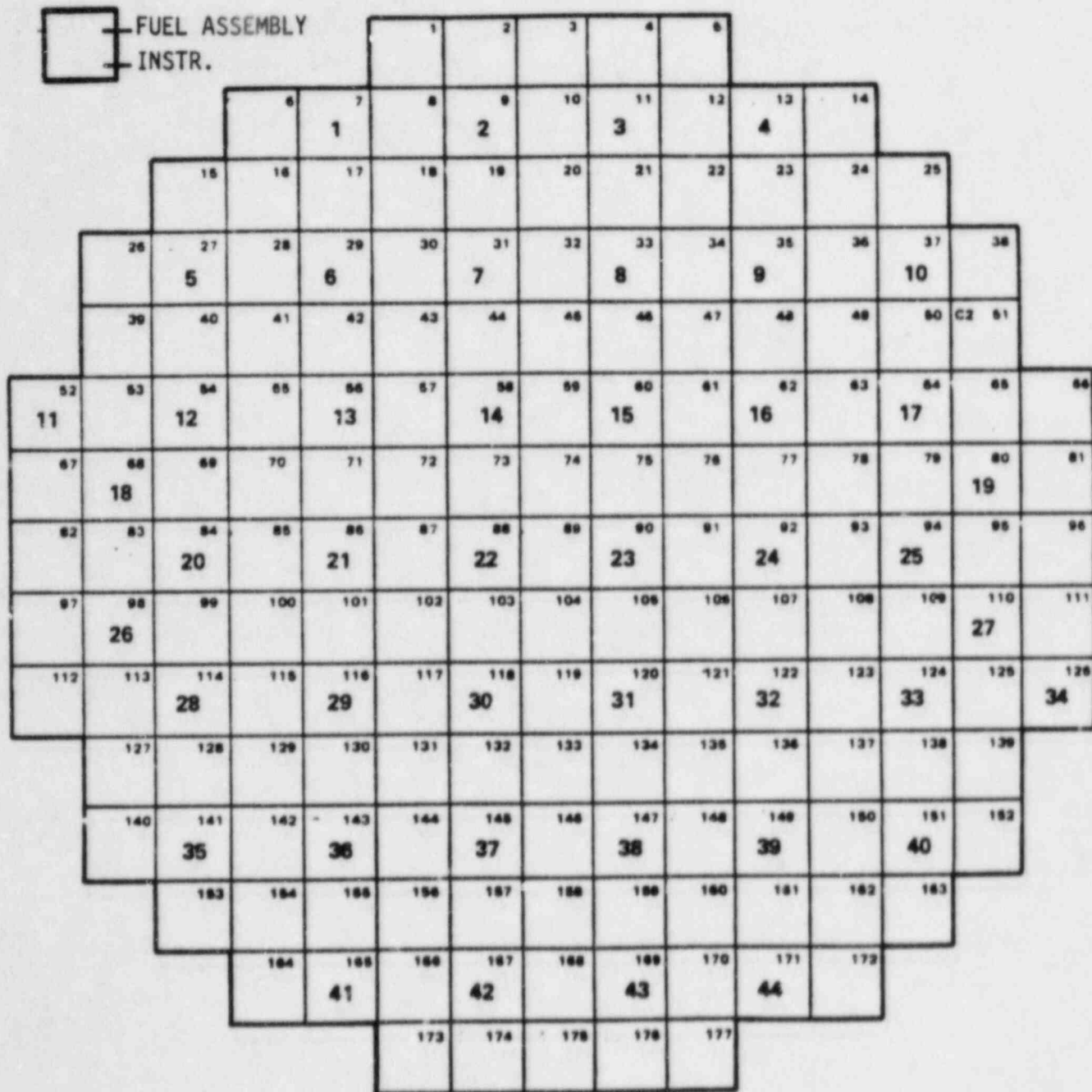
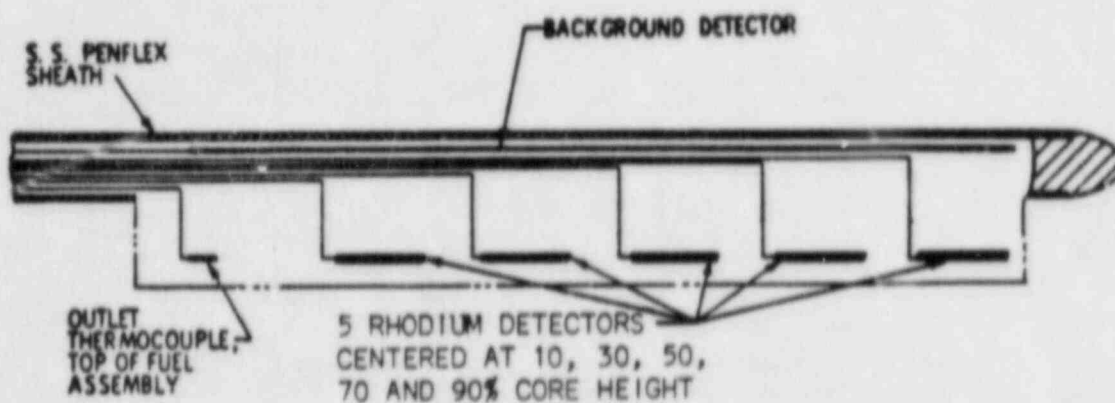


Figure 2.3

TYPICAL NEUTRON DETECTOR AND DETECTOR ASSEMBLY



TYPICAL INSTRUMENT ASSEMBLY



TYPICAL RHODIUM DETECTOR

Figure 2.4 RHODIUM EMITTER DECAY SCHEME

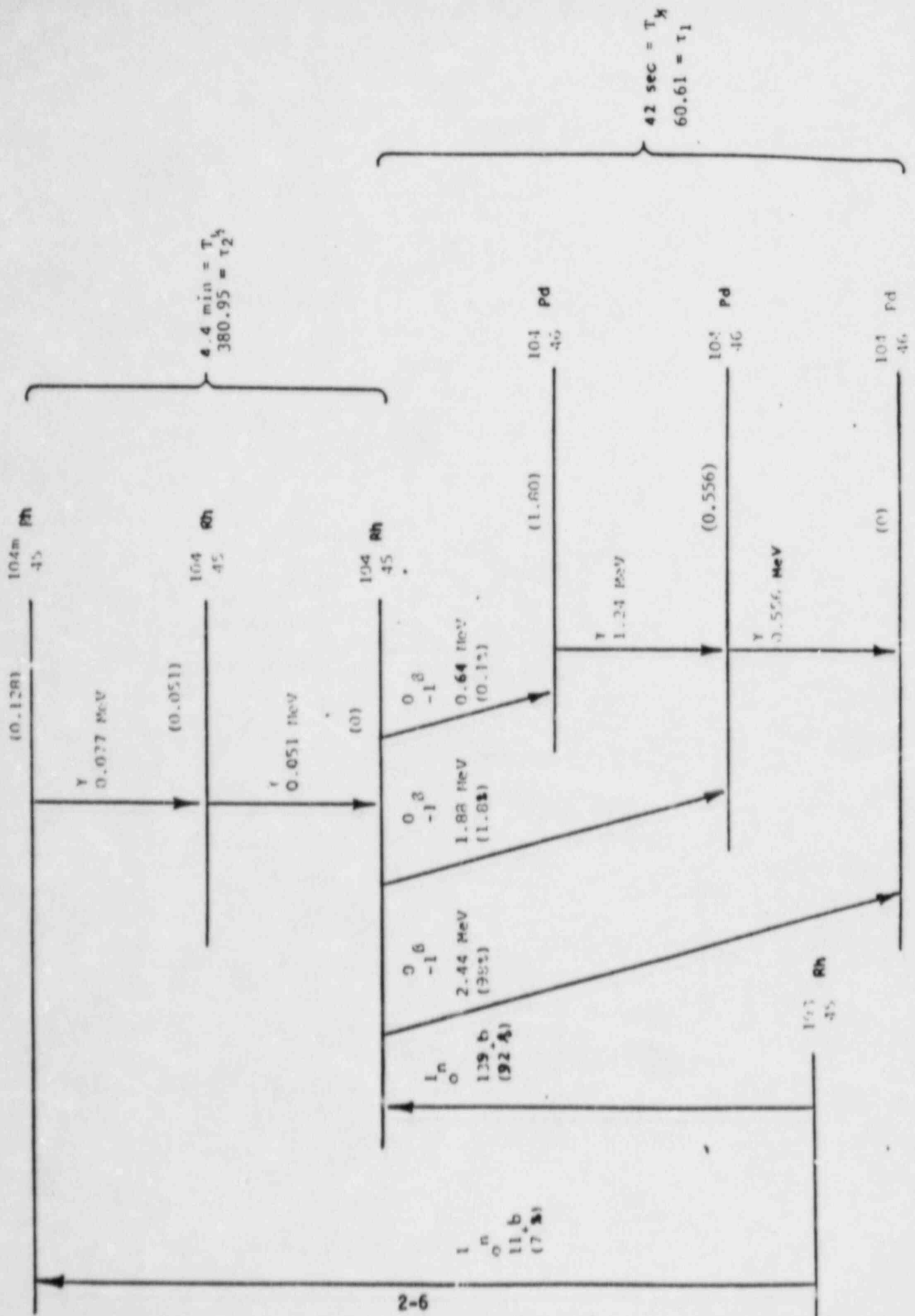
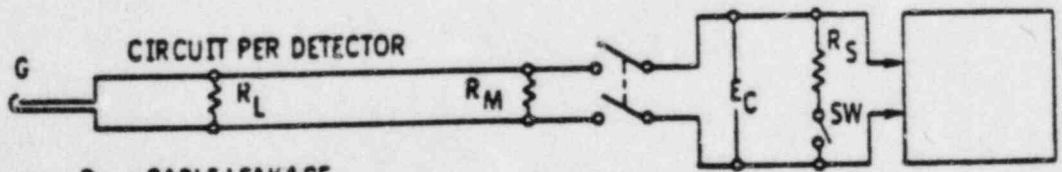
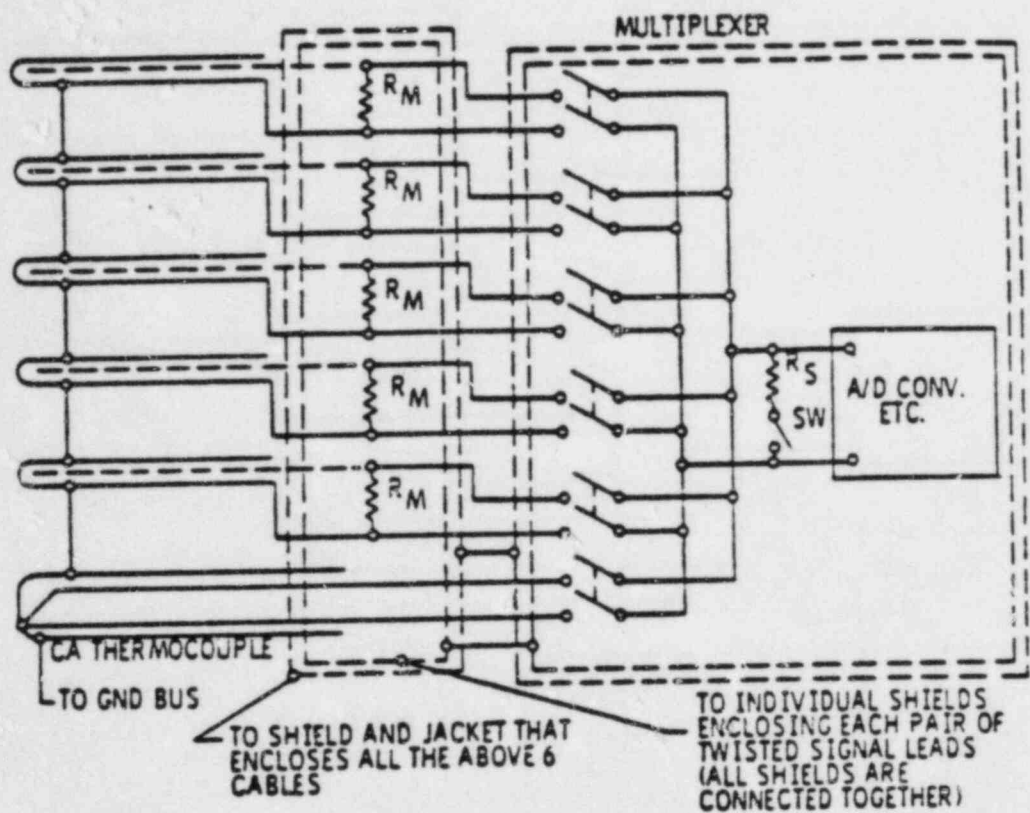


Figure 2.5

IN-CORE INSTRUMENTATION WIRING DIAGRAM



- R_L = CABLE LEAKAGE
- R_M = DETECTOR MEASURING RESISTANCE (e.g. $50 \times 10^3 \Omega$)
- R_S = SPECIAL RESISTOR (e.g. $20 \times 10^3 \Omega$)

3.0 CECOR POWER DISTRIBUTION CALCULATION

3.1 General

The CECOR program synthesizes 3-D power distributions from fixed incore detector readings. The first step in the process is to convert the signals from the five axially spaced detectors in a string to powers. Coupling coefficients are next used to calculate pseudo-detector powers in uninstrumented assemblies or assemblies with failed detectors. A five term Fourier fit is used to construct assembly axial shapes based on the five detector powers. Calculation of the maximum 1-pin and 4-pin assembly peaks are done using 1-pin and 4-pin peaking library coefficients. Libraries are a function of burnup and control rod position. The following sections present the MSS methodology for determining the flux-to-power conversion library, coupling coefficient library and 1-pin peaking factor libraries.

3.2 Flux-to-Power Conversion

The flux-to-power conversion factors are used to convert from depletion corrected instrument flux to assembly power integrated over detector length. The equation used is:

$$P_{in} = I_{in} IF_{in} \quad 3.2.1$$

Where P_{in} is the power for assembly i at detector level n and

I_{in} is the background and depletion corrected incore detector flux reading, and

IF_{in} is the flux-to-power conversion factor.

The flux-to-power factors (IF_{in}) are updated for each reload and are defined as the assembly power integrated over detector length divided by the rhodium reaction rate per rhodium atom.

A 2-D, 1/4 core PDQ depletion calculation is used to obtain both the assembly power and flux in the detector region used in IF_{in} . The PDQ model is that described in Reference 2 and is a two energy group model with each fuel pin modeled explicitly. All exterior regions which affect the power distribution are modeled including core baffle and reflector.

Effective rhodium absorption cross sections for use with PDQ fluxes are obtained by matching rhodium reaction rates from a PDQ assembly calculation to a detailed two-dimensional transport theory calculation with the CPM code (Reference 2). The transport theory calculation is an assembly depletion with the rhodium incore detector modeled explicitly. The rhodium is allowed to deplete. Two-group rhodium absorption cross sections for use with PDQ fluxes edited over the instrument cell are fit as a function of detector burnup.

Fast and Mixed Number Density (MND) thermal rhodium cross sections are combined with fast neutron flux and thermal neutron densities edited over instrument cells from the quarter core PDQ calculations to obtain rhodium reaction rates per atom. The assembly edits of power fraction are divided by rhodium reaction rates per atom to obtain the IF as shown in equation 3.2.2.

$$IF_{in} = \frac{P_{in}}{\int_E \int_V \sigma_a^{Rh} \phi \, dr \, dE} \quad 3.2.2$$

The IF_{in} coefficients are fit by cubic expressions in assembly cycle burnup.

3.3 Coupling Coefficients

Coupling coefficients relate the detector powers in instrumented assemblies to pseudo-detector powers in uninstrumented assemblies. Coupling coefficients are obtained from the 2-D 1/4 PDQ depletion calculations or from a 3-D nodal calculation. The coupling calculation is done prior to the axial synthesis described in Section 3.4. The coupling coefficient for assembly j is defined as:

$$CC_j = \sum_{i=1}^{N_j} P_i / (N_j * P_j) \quad 3.3.1$$

Where N_j is the number of assemblies neighboring assembly j

P_i are the powers in the neighboring assemblies at a specific detector level, and

P_j is the power in assembly j at the same detector level.

Coupling coefficients are generated for both rodged and unrodged core configurations and are fit by cubic expression versus assembly burnup.

3.4 Axial Power Synthesis

The axial power distribution synthesis converts the five incore detector level readings into a 51 node axial power shape using a Fourier fit as described in Reference 1. The choice of the input variable (wave number B) is the only required calculation. MSS uses a location and burnup dependent value of B based on 3-D nodal calculations.

3.5 One Pin Peaking Factor

The one pin peaking factor is defined as the ratio of the maximum pin power in an assembly to the average pin power in the assembly. One pin peaking factors are obtained from a 1/4 ccre PDQ full power depletion model. The one pin peaking factors are input to CECOR as cubic fits as a function of assembly burnup for each assembly and rod configuration.

3.6 4-Pin Peaking Factor

The 4-pin peaking factor is defined as the ratio of the maximum channel power in an assembly to the average power in the assembly. CECOR used to use the results of the 4-pin peaking calculation to pass to another program to calculate DNBR. Currently however, the one-pin peaking information is used for this purpose. MSS, therefore, supplies dummy data for the 4-pin peaking factor. If in the future the 4-pin peaking data is needed, the methodology will be identical to that for the 1-pin factors as described in Section 3.5.

4.0 CECOR LIBRARY GENERATION

Most of the information necessary to generate the CECOR data library comes from two dimensional, quarter core, full power, PDQ7 depletion calculations or 3-D nodal calculations. Both control rod out (ARO) and rods inserted calculations are performed.

A schematic of the CECOR library generation methodology is shown in Figure 4.1. Inputs are generated by the PDQ (Reference 4) and 3-D nodal simulator programs. The outputs include the CECOR cycle dependent data libraries as well as files used for quality assurance of the library. Output also includes graphs of the evaluated polynomial fits of the coefficients. Figure 4.2 is an example of the coupling coefficient for assembly #15 for ANO-2, Cycle 1. "B" designates the data points to be fitted and "A" designates the points calculated using the polynomial fit based on the "B" input points. These graphs serve to verify a smooth, well behaved fit between the input points.

FIGURE 4.1 SCHEMATIC OF CECOR LIBRARY GENERATION

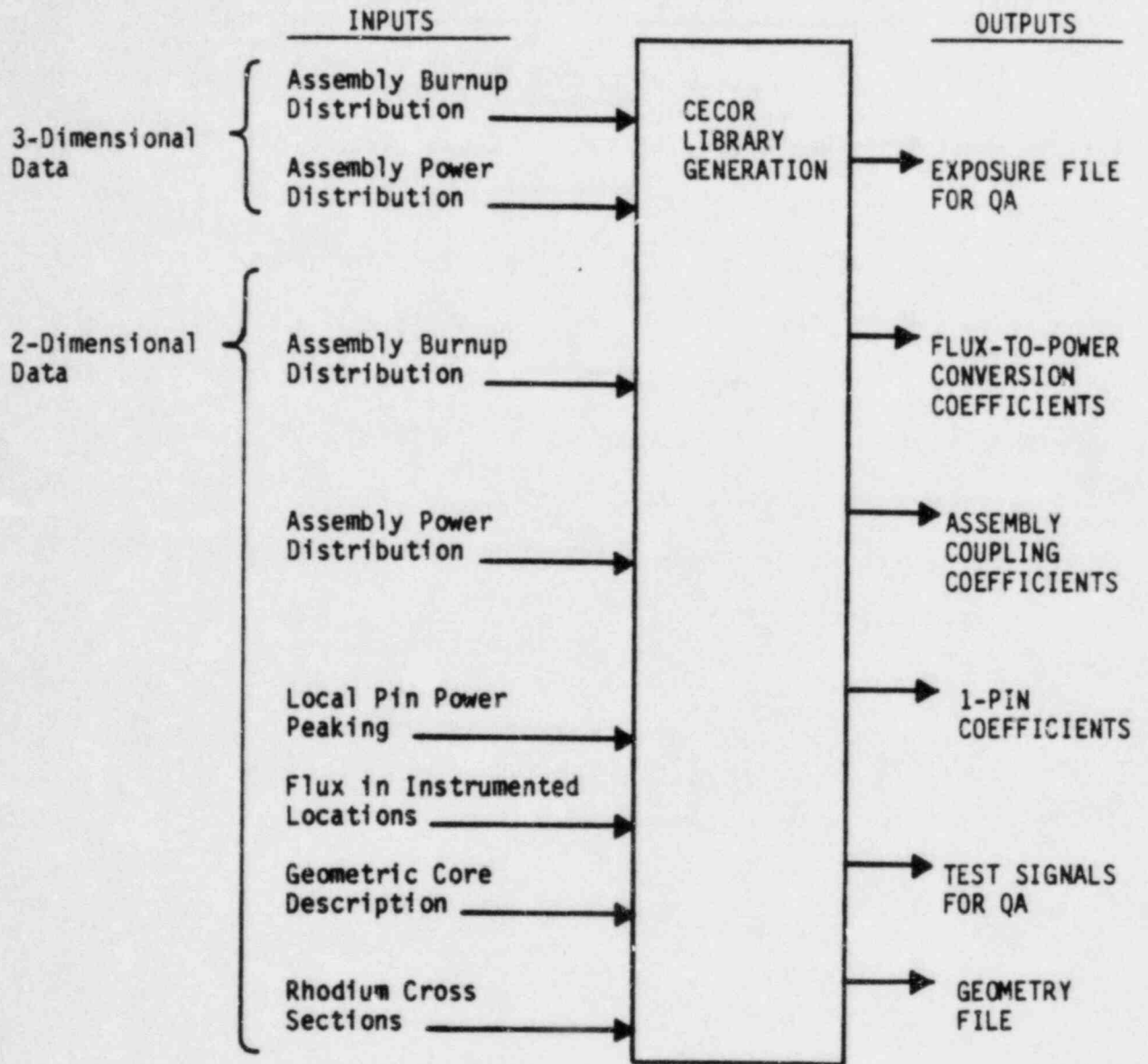
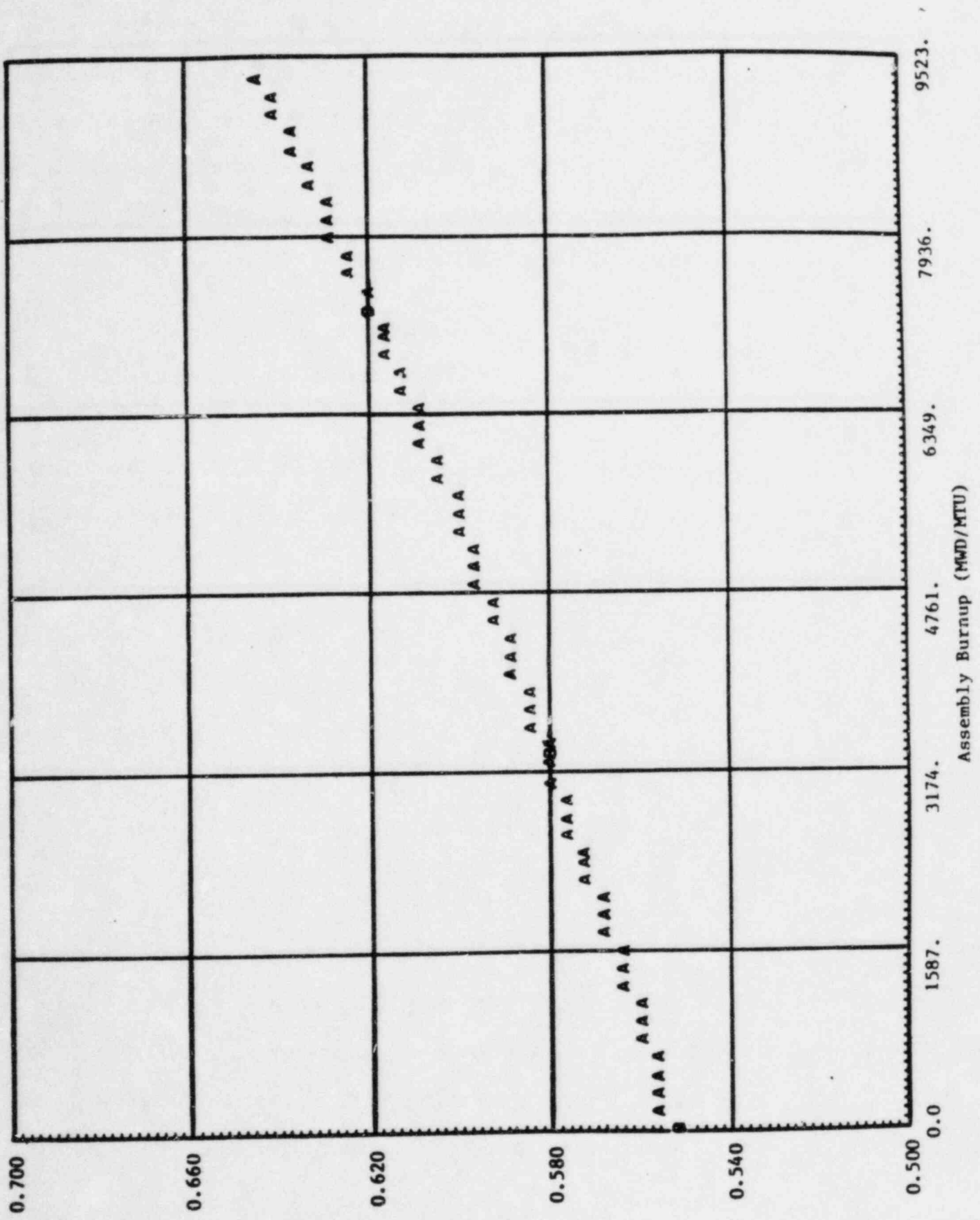


Figure 4.2 ASSEMBLY 15 COUPLING COEFFICIENT COMPARISON



5.0 DETERMINATION OF CECOR UNCERTAINTIES

5.1 General

The CECOR power distribution uncertainty relating to F_{xy} , F_r and F_q which are defined in Appendix A of this report is composed of four components which are discussed in detail in the following sections. The four are identified as the Coupling/Measurement Uncertainty, Assembly Axial Synthesis Uncertainty, Pin Peaking Synthesis Uncertainty and Pin Peaking Computational Uncertainty.

5.2 Coupling/Measurement Uncertainty

The Coupling/Measurement Uncertainty is the uncertainty associated with the measurement of power at the five detector levels. It includes uncertainties in the measured power in instrumented levels and the uncertainties in extrapolating to uninstrumented assemblies. [

The variable X is defined differently for F_q , F_r , and F_{xy} . For the purpose of quantifying F_q uncertainty, the variable X is defined as the power in any instrumented segment. For F_r the variable X is defined as the sum of five detector segments in any assembly. For F_{xy} the

variable X is the power at any instrumented segment within a core level.

Data from two different size plants was included, three cycles of data for a 177 FA plant and one cycle of data for a 217 FA plant. The 217 fuel assembly plant is San Onofre Unit 2 which has the same reactor core as Waterford-3. Tables 5.2.1 - 5.2.4 are a list of the CECOR cases run to calculate the Coupling/Measurement Uncertainty. Tables 5.2.5 through 5.2.8 provide a summary of the statistics from the four cycles of comparisons.

The resultant map-by-map and cycle-by-cycle statistics were pooled. A poolability test was performed before pooling. In the event the data did not pass the poolability test, a conservative measure was taken as described in Appendix B.

5.3 Assembly Axial Synthesis Uncertainty

The axial synthesis of the detailed three dimensional assembly power distribution is done in the CECOR program using a Fourier series expansion. Three dimensional nominal cycle nodal code depletions as well as rodded cases are performed and the nodal power distributions obtained are used to generate CECOR input detector signals. The accuracy of the CECOR axial synthesis (Fourier fit) is then determined by comparing the Fourier fit to the original nodal code calculation.

After normalization of the CECOR total core power to the nodal core power, three different errors are calculated from the nodal and fit power distribution comparisons:

1. The relative difference between the nodal code and Fourier fit values of integrated power for each assembly.
2. The relative difference between the nodal code and fit values of assembly axial peak to core average power density for each assembly.
3. The relative difference between the nodal code and fit values of the maximum assembly planar power to the plane average power for each plane.

These quantities are used in the calculation of the F_r , F_q and F_{xy} uncertainties, respectively. Appendix D gives a comparison of synthesized power distributions in the assembly containing the peak F_q vs. the nodal input powers for both reactors at several points in each cycle. Comparisons are performed for all assemblies in the calculation of the F_r and F_q uncertainties and for all nodal planes used in the calculation of the F_{xy} . Table 5.3-1 gives a list of the cases used in the development of the assembly axial synthesis uncertainty and the resulting standard deviation and mean error. The F_q and F_r statistics comprise 177 (217 for W-3) comparisons per case and F_{xy} comprises 12 comparisons per case. All statepoints are at one hundred percent (100%) full power. Since the errors were found to be non-normal, a non parametric, one sided tolerance limit was calculated and a $K_{95/95}$ value

was then obtained from Reference 7 for the number of samples available. A standard deviation was then calculated to conserve the one-sided tolerance limit. Figures 5.3.1-3 give comparisons of the sample error distributions and the normal distributions with the calculated standard deviations. As can be seen in the figures, the normal distribution tolerance limit bounds the sample error distributions except for very small percents shown in the figures, indicating that the normal assumption is conservative.

5.4 Pin Peaking Synthesis Uncertainty

CECOR pin peaking libraries are generated from a PDQ model which models a slice through the reactor core at one particular level. MSS uses an "average" power plane. The Pin Peaking Synthesis Uncertainty is the uncertainty associated with the pin peaking at axial heights other than this "average" power plane. MSS estimates the pin peaking synthesis error from a comparison of PDQ results [

] The deviations in the calculated pin peaking between these [] correspond to the maximum overall deviations within the instrumented portion of core height. Figures 5.4-1 through 5.4-2 give the comparisons of the PDQ power distributions [] for rodged and unrodged cases.

5.5 Pin Peaking Computational Uncertainty

Since the local pin power cannot be measured directly in the operating reactor, the pin power synthesis process must rely on calculated values of pin-to-box factors. The pin peaking computational uncertainty is the uncertainty associated with the PDQ calculation of pin-to-box peaking factors. The MSS pin peaking computational uncertainties were based on PDQ comparisons to CPM calculations which were compared to critical experiments. The MSS pin peaking computational uncertainties were documented in the physics methodology report (Reference 2). The pin factor uncertainty established in Reference 2 was [

]

5.6 Combination of Uncertainties

In order to determine a lower tolerance limit for the random error in pin peaking factors F_q , F_r , and F_{xy} as measured by CECOR, it is necessary to statistically combine the uncertainty factors due to Coupling/Measurement (C/M), Assembly Axial Synthesis (AAS), Pin Peaking Synthesis (PPS) and Pin Peaking Calculations (PPC). Since the error components are due to entirely different and unrelated factors, they are independent and uncorrelated random variables, and one may write:

$$\mu = \mu_{C/M} + \mu_{AAS} + \mu_{PPS} + \mu_{PPC} \quad 5.6.1$$

and

$$\sigma^2 = \sigma_{C/M}^2 + \sigma_{AAS}^2 + \sigma_{PPS}^2 + \sigma_{PPC}^2 \quad 5.6.2$$

Using the sample means and variances from Sections 5.2 - 5.5 as estimates of the true bias and variance, one can write:

$$\mu \approx \bar{D} = \bar{D}_{C/M} + \bar{D}_{AAS} + \bar{D}_{PPS} + \bar{D}_{PPC} \quad 5.6.3$$

and

$$\sigma^2 \approx S^2 = S_{C/M}^2 + S_{AAS}^2 + S_{PPS}^2 + S_{PPC}^2 \quad 5.6.4$$

The sample statistics \bar{D} and S from equations 5.6.3 and 5.6.4 are estimates of the true parameters μ and σ and are therefore subject to a random distribution of their own. The one sided lower tolerance limit can be calculated such that the uncertainty in the CECOR power can be estimated on a 95%/95% probability/confidence level.

Table 5.6.1 lists the estimates of \bar{D} and S and the number of degrees of freedom of the four components of CECOR pin power uncertainty. If one expresses the sample variance as being proportional to a χ^2 distribution, one may write:

$$S^2 = \frac{\chi^2 \sigma^2}{f} \quad 5.6.5$$

or substituting in equation 5.6.4, one can write:

$$\frac{\chi^2 \sigma^2}{f} = \frac{\chi^2 \sigma_{C/M}^2}{f_{C/M}} + \frac{\chi^2 \sigma_{AAS}^2}{f_{AAS}} + \frac{\chi^2 \sigma_{PPS}^2}{f_{PPS}} + \frac{\chi^2 \sigma_{PPC}^2}{f_{PPC}} \quad 5.6.6$$

and taking the variance of both sides

$$\frac{2f\sigma^4}{f^2} = \frac{2f_{C/M} \sigma_{C/M}^4}{f_{C/M}^2} + \frac{2f_{AAS} \sigma_{AAS}^4}{f_{AAS}^2} + \frac{2f_{PPS} \sigma_{PPS}^4}{f_{PPS}^2} + \frac{2f_{PPC} \sigma_{PPC}^4}{f_{PPC}^2} \quad 5.6.7$$

or:

$$\frac{\sigma^4}{f} = \frac{\sigma_{C/M}^4}{f_{C/M}} + \frac{\sigma_{AAS}^4}{f_{AAS}} + \frac{\sigma_{PPS}^4}{f_{PPS}} + \frac{\sigma_{PPC}^4}{f_{PPC}} \quad 5.6.8$$

Using the sample variances as approximations for the true variances, one can write:

$$f = \frac{S^4}{\frac{S_{C/M}^4}{f_{C/M}} + \frac{S_{AAS}^4}{f_{AAS}} + \frac{S_{PPS}^4}{f_{PPS}} + \frac{S_{PPC}^2}{f_{PPC}}} \quad 5.6.9$$

where all measured variances are known. The number of degrees of freedom is used to determine the lower one-sided tolerance limit for the 95%/95% probability/confidence interval. The results for F_q , F_{xy} and F_r are given in Table 5.6.2. These tolerance limits insure that there is a 95% probability that at least 95% of the true F_{xy} , F_r and F_q will be less than the F_{xy} , F_r and F_q measured by CECOR plus 6.92, 5.69, and 7.71% respectively.

TABLE 5.2.1 ANO2 CYCLE 1 CECOR STATEPOINTS

<u>CASE #</u>	<u>EXPOSURE (MWD/MT)</u>	<u>POWER</u>	<u>CONTROL ROD BANK (% INSERTED)</u>		
			<u>5</u>	<u>6</u>	<u>PLR</u>
1	2544	99.5	0	0	0
2	3208	99.9	0	0	0
3	4385	89.0	0	0	0
4	5916	100.0	0	0	0
5	6750	100.0	0	0	0
6	8012	100.0	0	0	0

TABLE 5.2.2 ANO2 CYCLE 2 CECOR STATEPOINTS

<u>CASE #</u>	<u>EXPOSURE (MWD/MT)</u>	<u>POWER</u>	<u>CONTROL ROD BANK (% INSERTED)</u>		
			<u>5</u>	<u>6</u>	<u>PLR</u>
1	7975	50.7	0	6	0
2	8242	72.2	0	0	0
3	8959	96.8	0	6	0
4	9282	95.3	0	0	0
5	9505	97.3	0	7.5	0
6	10013	99.7	0	0	0
7	10140	77.6	0	6	0
8	11589	100.0	0	0	0
9	12394	99.6	0	0	0
10	13986	100.0	0	0	0
11	14276	99.6	0	4.5	0
12	14745	89.7	0	0	0
13	15932	99.9	0	0	0
14	18200	99.3	0	3.4	0
15	18646	84.4	0	3.2	0
16	18971	76.1	0	0	0
17	7975	49.9	0	96.5	0
18	7975	49.6	68.6	96.5	0
19	7975	50.4	67.9	96.9	0
20	7975	49.7	0	96.9	73.2
21	7975	50.2	0	0	73.2

TABLE 5.2.3 ANO2 CYCLE 3 CECOR STATEPOINTS

<u>CASE #</u>	<u>EXPOSURE (MWD/MT)</u>	<u>POWER</u>	<u>CONTROL ROD BANK (% INSERTED)</u>		
			<u>5</u>	<u>6</u>	<u>PLR</u>
1	11183	50.1	0	0	0
2	11243	49.6	0	0	0
3	11601	80.1	0	0	0
4	12537	99.7	0	0	0
5	14026	92.8	0	0	0
6	14965	99.8	0	0	0
7	15152	100.0	0	0	0
8	11183	50.4	97.4	97.4	0
9	11183	49.7	97.4	97.4	74.6
10	11183	50.3	0	97	74.6
11	11183	50.7	0	97	0

TABLE 5.2.4 217 FA CYCLE 1 CECOR STATEPOINTS

<u>CASE #</u>	<u>EXPOSURE (MWD/MT)</u>	<u>POWER</u>	<u>CONTROL ROD BANK (% INSERTED)</u>		
			<u>5</u>	<u>6</u>	<u>PLR</u>
1	979	80.4	0	0	0
2	1599	91.1	0	0	0
3	1884	96.0	0	0	0

TABLE 5.2.5 ANO-2 CYCLE 1 CECOR STATISTICS

CASE	FX Y LEVEL=1			FX Y LEVEL=2			FX Y LEVEL=3			FX Y LEVEL=4		
	$\bar{D}(X)$	S(X)	N	$\bar{D}(X)$	S(X)	N	$\bar{D}(X)$	S(X)	N	$\bar{D}(X)$	S(X)	N
1			42			42			42			40
2			42			42			43			41
3			43			42			43			42
4			43			43			42			42
5			42			43			42			42
6			44			43			42			42

CASE	FX Y LEVEL=5			$\bar{D}(X)$	FR S(X)	N	$\bar{D}(X)$	FG S(X)	N
	$\bar{D}(X)$	S(X)	N						
1			41			36			207
2			42			38			210
3			43			39			213
4			43			39			213
5			43			38			212
6			43			39			214

TABLE 5.2.6 ANO-2 CYCLE 2 CECOR STATISTICS

CASE	FXV LEVEL=1			FXV LEVEL=2			FXV LEVEL=3			FXV LEVEL=4		
	$\bar{D}(X)$	S(X)	N	$\bar{D}(X)$	S(X)	N	$\bar{D}(X)$	S(X)	N	$\bar{D}(X)$	S(X)	N
1			43			44			44			44
2			43			44			44			44
3			44			44			44			42
4			44			44			44			42
5			44			44			44			42
6			44			44			44			42
7			44			44			44			42
8			42			43			43			42
9			42			43			43			42
10			42			43			43			42
11			42			43			43			42
12			43			43			43			42
13			42			43			43			42
14			42			42			43			42
15			41			40			41			41
16			40			40			39			42
17			42			42			42			42
18			42			42			42			42
19			41			42			42			42
20			41			42			42			42
21			41			42			42			42

CASE	FXV LEVEL=5			FR			FG		
	$\bar{D}(X)$	S(X)	N	$\bar{D}(X)$	S(X)	N	$\bar{D}(X)$	S(X)	N
1			42			41			217
2			42			41			217
3			42			42			216
4			42			42			216
5			42			42			216
6			42			42			216
7			42			42			216
8			42			41			212
9			42			41			212
10			42			41			212
11			42			41			212
12			42			42			213
13			42			41			212
14			42			40			211
15			41			38			204
16			39			36			200
17			42			42			210
18			42			42			210
19			42			41			209
20			42			41			209
21			42			41			209

TABLE 5.2.7 ANO-2 CYCLE 3 CECOR STATISTICS

CASE	FXV LEVEL=1			FXV LEVEL=2			FXV LEVEL=3			FXV LEVEL=4		
	$\bar{D}(X)$	S(X)	N	$\bar{D}(X)$	S(X)	N	$\bar{D}(X)$	S(X)	N	$\bar{D}(X)$	S(X)	N
1			40			38			33			38
2			40			38			33			38
3			40			38			33			38
4			40			37			33			38
5			40			37			33			38
6			40			37			33			38
7			40			37			33			38
8			39			37			32			37
9			39			37			32			37
10			39			37			32			37
11			39			37			32			37

CASE	FXV LEVEL=5			FR			FC		
	$\bar{D}(X)$	S(X)	N	$\bar{D}(X)$	S(X)	N	$\bar{D}(X)$	S(X)	N
1			38			31			187
2			38			31			187
3			37			30			186
4			37			30			185
5			36			30			184
6			38			31			186
7			37			31			185
8			37			30			182
9			37			30			182
10			37			30			182
11			37			30			182

TABLE 5.2.8 217 FA CYCLE 1 CECOR STATISTICS

CASE	FX Y LEVEL=1			FX Y LEVEL=2			FX Y LEVEL=3			FX Y LEVEL=4		
	$\bar{D}(X)$	S(X)	N	$\bar{D}(X)$	S(X)	N	$\bar{D}(X)$	S(X)	N	$\bar{D}(X)$	S(X)	N
1			56			56			55			56
2			56			56			55			56
3			56			56			56			55

CASE	FX Y LEVEL=5			FR			FQ		
	$\bar{D}(X)$	S(X)	N	$\bar{D}(X)$	S(X)	N	$\bar{D}(X)$	S(X)	N
1			56			55			279
2			56			55			279
3			56			55			279

TABLE 5.3.1 ASSEMBLY AXIAL SYNTHESIS UNCERTAINTY

S-16

	EXPOSURE MWD/MT	RODS	F _Q		F _{XY}		FR	
			$\%S$	$\%D$	$\%S$	$\%D$	$\%S$	$\%D$
ANO2C2	0	ARO						
ANO2C2	500	ARO						
ANO2C2	1000	ARO						
ANO2C2	2000	ARO						
ANO2C2	3000	ARO						
ANO2C2	4000	ARC						
ANO2C2	5000	ARO						
ANO2C2	6000	ARO						
ANO2C2	7000	ARO						
ANO2C2	8000	ARC						
ANO2C2	9000	ARC						
ANO2C2	10000	ARO						
ANO2C2	11000	ARC						
ANO2C2	0	6						
ANO2C2	1362	6						
ANO2C2	4705	6						
ANO2C2	7528	6						
ANO2C2	10500	6						
ANO2C2	0	665						
ANO2C2	1362	665						
ANO2C2	4705	665						
ANO2C2	7528	665						
ANO2C2	10500	665						
ANO2C2	0	P						
ANO2C2	1362	P						
ANO2C2	4705	P						
ANO2C2	7528	P						
ANO2C2	10500	P						

TABLE 5.3.1 ASSEMBLY AXIAL SYNTHESIS UNCERTAINTY

PAGE -2-

	EXPOSURE MWD/MT	RODS	FQ		FXY		FR		
			$\%S$	$\%D$	$\%S$	$\%D$	$\%S$	$\%D$	
ANO2C2	0	P86	[]
ANO2C2	1362	P86							
ANO2C2	4705	P86							
ANO2C2	7528	P86							
ANO2C2	10500	P86							
ANO2C2	0	P,685							
ANO2C2	1362	P,685							
ANO2C2	4705	P,685							
ANO2C2	7528	P,685							
ANO2C2	10500	P,685							
ANO2C3	0	ARC							
ANO2C3	500	ARC							
ANO2C3	1000	ARC							
ANO2C3	2000	ARC							
ANO2C3	3000	ARC							
ANO2C3	4000	ARC							
ANO2C3	5000	ARC							
ANO2C3	6000	ARC							
ANO2C3	7000	ARC							
ANO2C3	8000	ARC							
ANO2C3	9000	ARC							
ANO2C3	10000	ARC							
ANO2C3	11000	ARC							

S-17

TABLE 5.3.1 ASSEMBLY AXIAL SYNTHESIS UNCERTAINTY

PAGE -3-

5-18

	EXPOSURE	RODS	FZ		FXY		FR	
	MWD/MT		\bar{x}_S	\bar{x}_D	\bar{x}_S	\bar{x}_D	\bar{x}_S	\bar{x}_D
ANO2C3	0	6						
ANO2C3	1862	6						
ANO2C3	4705	6						
ANO2C3	7528	6						
ANO2C3	10500	6						
ANO2C3	0	635						
ANO2C3	1862	685						
ANO2C3	4705	635						
ANO2C3	7528	635						
ANO2C3	10500	635						
ANO2C3	0	P						
ANO2C3	1862	P						
ANO2C3	4705	P						
ANO2C3	7528	P						
ANO2C3	10500	P						
ANO2C3	0	P66						
ANO2C3	1862	P66						
ANO2C3	4705	P26						
ANO2C3	7528	P66						
ANO2C3	10500	P7665						
ANO2C3	0	P7635						
ANO2C3	1862	P7685						
ANO2C3	4705	P7625						
ANO2C3	7528	P7685						
ANO2C3	10500	P7635						
W3C1	12.5	ARO						

Figure 5.3.1 Fxy Assembly Axial Synthesis Error



Figure 5.3.2 Fr Assembly Axial Synthesis Error

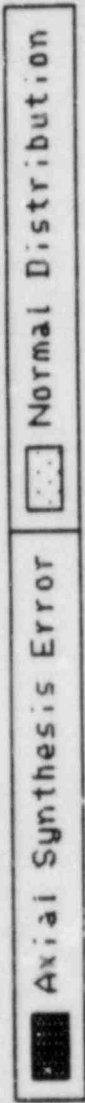
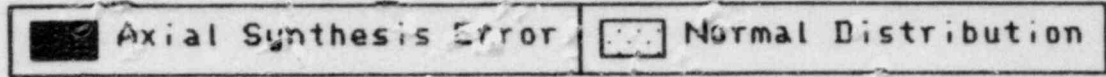


Figure 5.3.3 Fq Assembly Axial Synthesis Error



5-21

Figure 5.4.1 ANO-2 Cycle 2 BOC
Comparison of [Average Pin Power, ARO

] PDQ Peak Pin to Assembly

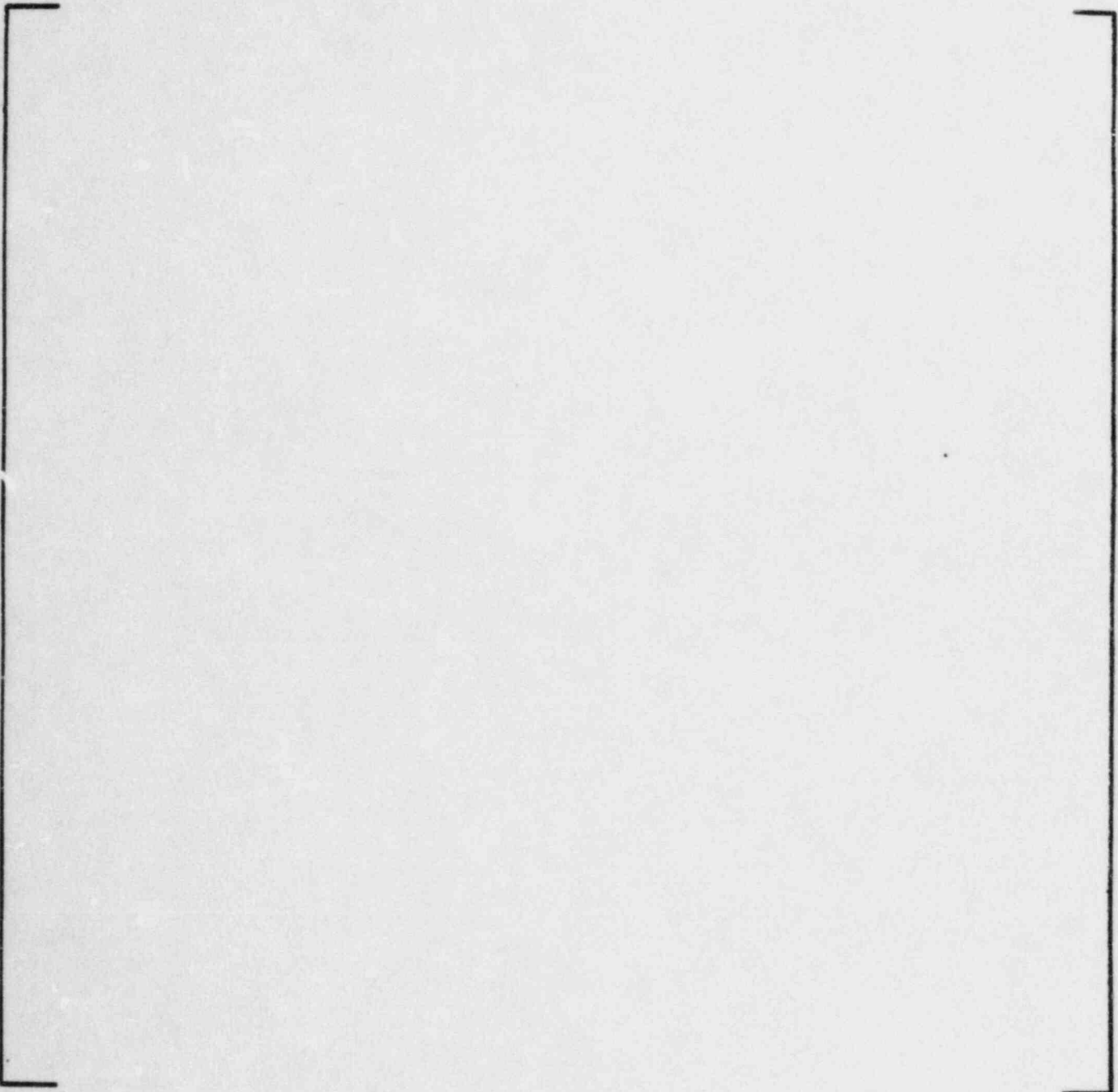


Figure 5.4.2 ANO-2 Cycle 2 BOC
Comparison of [Average Pin Power, BK6 Inserted

] PDQ Peak Pin to Assembly

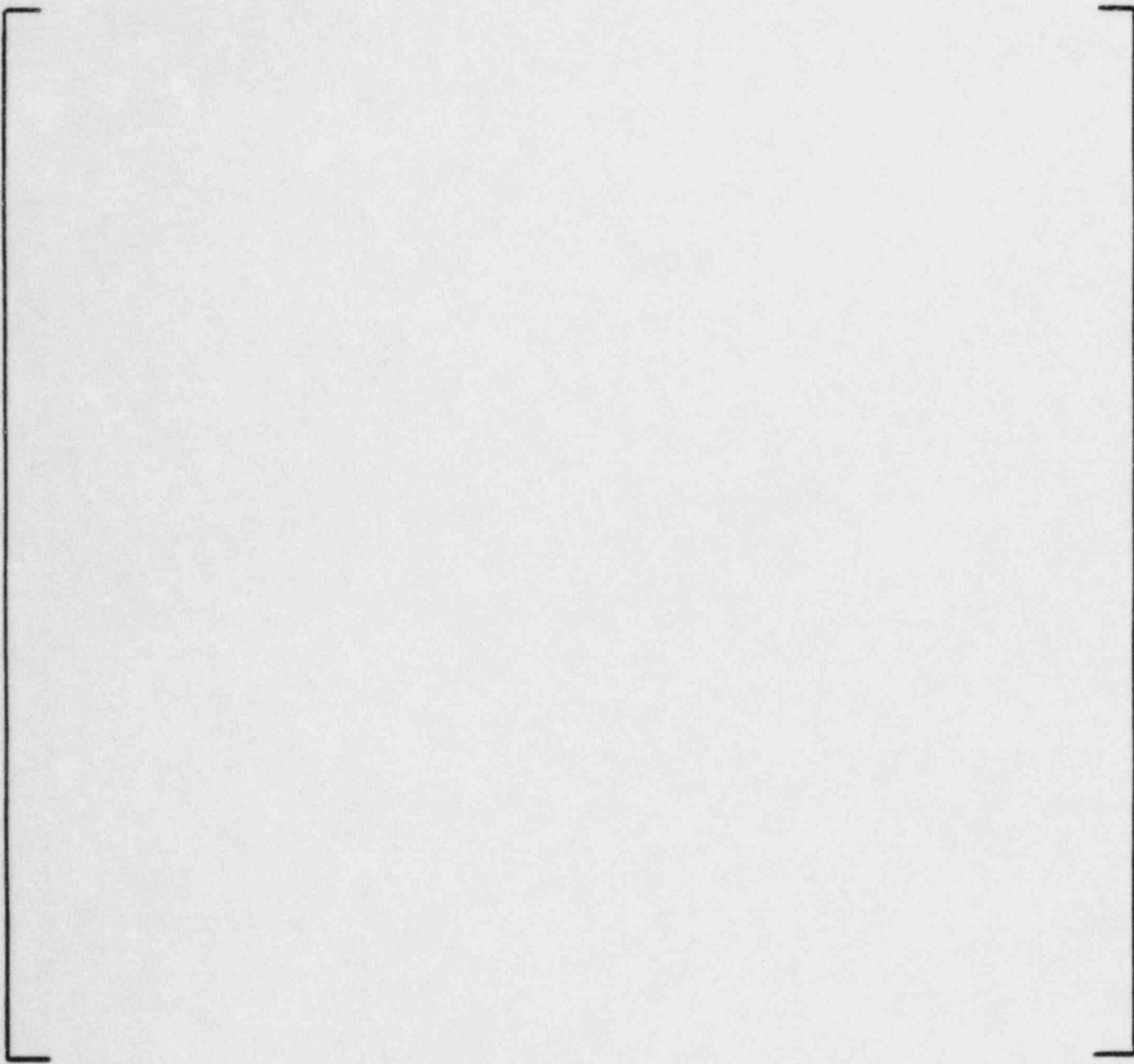


FIGURE 5.4.3 Pin Peaking Synthesis Error



TABLE 5.6.1
SUMMARY OF UNCERTAINTY COMPONENTS FOR
CECOR PEAKING FACTORS

<u>PARAMETER</u>	<u>UNCERTAINTY COMPONENT</u>	<u>D</u> <u>(%)</u>	<u>S</u> <u>(%)</u>	<u>n</u>	<u>k</u>	<u>D-kS</u>
Fxy	Coupling/Measurement					
	Assembly Axial Synthesis					
	Pin Power Synthesis					
	Pin Power Calculational					
Fr	Coupling Measurement					
	Assembly Axial Synthesis					
	Pin Power Synthesis					
	Pin Power Calculational					
Fq	Coupling Measurement					
	Assembly Axial Synthesis					
	Pin Power Synthesis					
	Pin Power Calculational					

TABLE 5.6.2
COMBINED 95%/95% PROBABILITY/CONFIDENCE
LOWER TOLERANCE LIMITS FOR
CORE PEAKING FACTORS MEASURED BY CECOR

<u>PARAMETER</u>	<u>D</u> <u>%</u>	<u>S</u> <u>%</u>	<u>f</u>	<u>k</u>	<u>D-kS</u> <u>%</u>
Fxy	[]]]	-6.92
Fr					-5.69
Fq					-7.71

6.0 REFERENCES

1. CECOR 2.0 General Description, Methods and Algorithms, NPSD-103-P, Combustion Engineering, 6/80.
2. Qualification of Reactor Physics Methods for Application to Pressurized Water Reactors of the Middle South Utilities System, MSS-NAT-P, 8/4/80.
3. INCA/CECOR Power Peaking Uncertainty, CENPD-153-P Revision 1-P-A, Combustion Engineering, 5/80.
4. B. M. Rothleder, PDQ7/HARMONY User's Manual, EPRI 8/1/79.
5. American National Standard Assessment of the Assumption of Normality, ANSI W15.15 - 1974.
6. W. J. Conover, Practical Non-Parametric Statistics, John Wiley and Sons, New York, 1980.
7. R. E. Odeh and D. B. Owen, Tables for Normal Tolerance Limits, Sampling Plans, and Screening, Marcel Dekker, Inc., New York, 1980.

APPENDIX A DEFINITION OF TERMS

1.0 F_q : The maximum 3-D power. One value for the core; i.e., the maximum for a nodal power (i.e., the maximum of any of (177/ANO-2, 217/W-3) XY assembly power values on any of the 51 Z planes) times the appropriate pin to assembly factor.

2.0 F_{xy} : Calculated for each axial plane as follows:

Let there be 51 axial nodes ($i = 1, 51$)

Let there be 177 assemblies ($j = 1, 177$) (W-3 = 217 assemblies)

a) Search for maximum P_j within that plane i

$$P_{jmax} = \text{Max of } [P_1, P_2, P_3 \dots P_{177}]_i$$

b) Find the average power for that plane i

$$\bar{P}_{ji} = \frac{1}{177} \sum_{j=1}^{177} P_{ji}$$

c) Increase P_{jmax} as defined in a) by the pin to assembly ratio to account for local peaking, i.e.

$$P_{jmax \text{ Local Peaked}} = P_{jmax} * (\text{pin to assembly ratio})$$

d) Then, define F_{xy} for that plane i

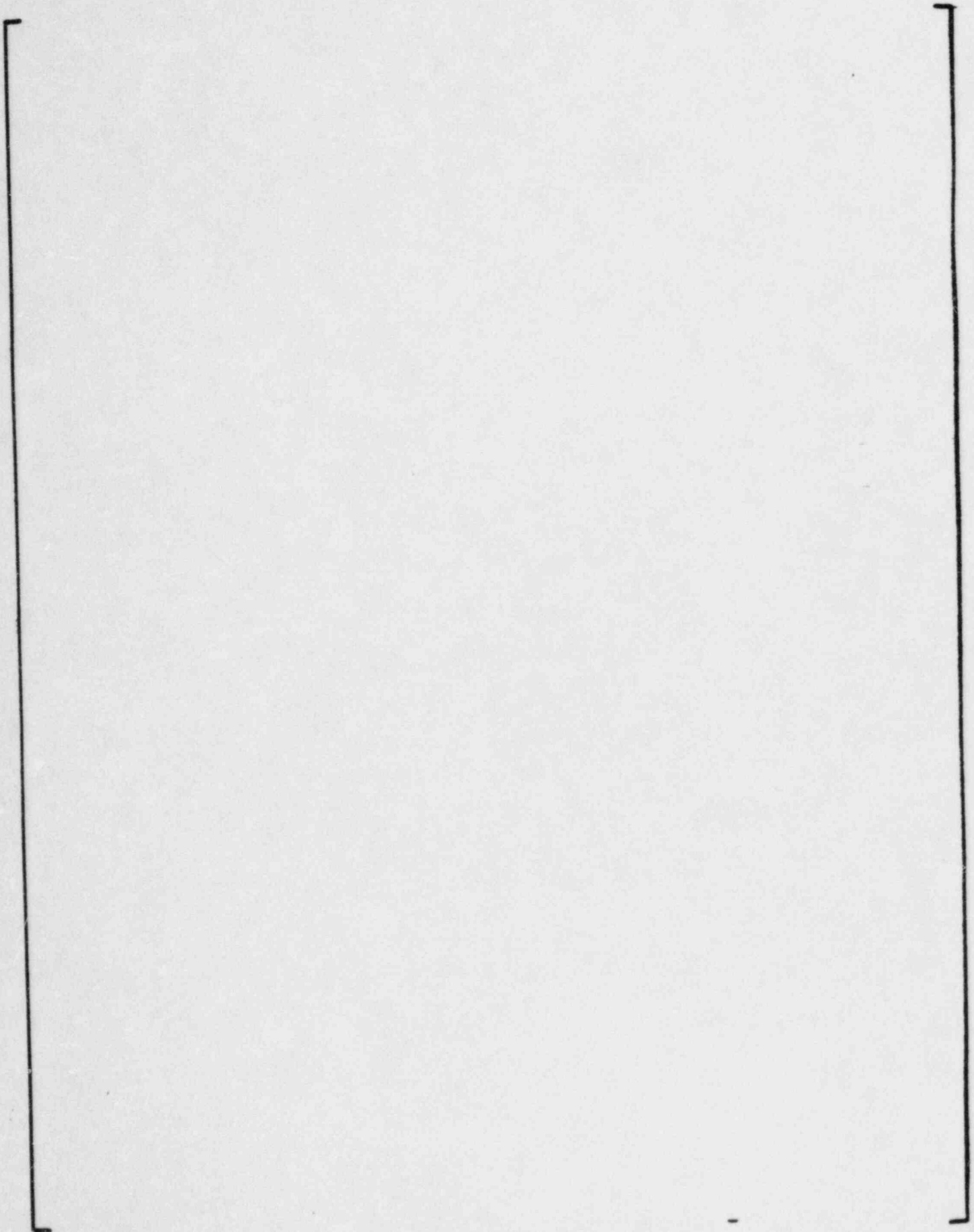
$$F_{xyi} = \frac{P_{jmax \text{ Local Peaked}}}{\bar{P}_{ji}}$$

3.0 F_r : Defined for any assembly as follows:

$$F_{rj} = \frac{1}{51} \sum_{i=1}^{51} P_{ji}$$

where P_{ji} is maximum pin power in assembly j at level i

APPENDIX B POOLING METHODOLOGY



APPENDIX C

COUPLING/MEASUREMENT ERRORS FOR
177 and 217 FUEL ASSEMBLY PLANTS

Figures C.1 - C-45

PROPRIETARY

APPENDIX D

ASSEMBLY AXIAL SYNTHESIS ERRORS FOR
177 AND 217 FUEL ASSEMBLY PLANTS

Figures D.1 - D.11

PROPRIETARY